Significant Improvement on the Electroluminescence Characteristics of MEH-PPV by Blending with PMMA

Ching-Shiun Chao[1], Wha-Tzong Whang[1,*] and Kuen-Ru Chuang[2]

1. *Department of Materials Science & Engineering, National Chiao Tung University, 1001 Ta Hsueh Road, Hsinchu 30010, Taiwan, Republic of China*
2. *Chemical Engineering Department, National Tsing-Hua University, Hsinchu 30013, Taiwan, Republic of China*

Received April 14, 2000; revised June 27, 2000; accepted July 10, 2000

Abstract: A significant improvement on the electroluminescence threshold voltage from 5.5 volts down to 2.9 volts of poly[2-methoxy-5-(2-ethylhexyloxy)-1,4-phenylene vinylene] (MEH-PPV) in the Ca/polymer/ITO diode is observed by incorporating a non-conjugated PMMA into MEH-PPV. The threshold voltage of the material decreases with the poly(methyl methacrylate) (PMMA) content. Near-field scanning absorption and photoluminescence micrographs show that the PMMA domains dispersed in the continuous MEH-PPV phase appear to be similar to sesame seeds embedded in the MEH-PPV pancakes. The resistivity of PMMA is two orders lower than that of MEH-PPV. The excellent electrical conduction of PMMA in Ca/PMMA/ITO glass devices is not due to a pin-hole defect mechanism but may result from the electron hopping from Ca through the carbonyl groups in the PMMA. The significant improvement in the threshold voltage may be due to the combination of the electron hopping in the thin PMMA sesame seeds and the thinner thickness effect of MEH-PPV in the light emitting layer.

Keywords: Poly[2-methoxy-5-(2-ethylhexyloxy)-1,4-phenylene vinylene] (MEH-PPV), Poly(methyl methacrylate) (PMMA), Light emitting diode, Near-field scanning optical micrographs (NSOM), Electroluminescence.

Introduction

Since the first polymer light emitting diode (PLED) of poly(p-phenylene vinylene) was reported by the Cambridge group [1], many conjugated polymers or organic compounds have been studied as light emitting related materials. Much effort has been put forth to adjust the emitting light wavelength, to improve the light emitting quantum efficiency, and to promote the lifetime of the PLEDs [2-4]. The emitting light wavelength is primarily related to the energy gap between the lowest unoccupied molecular orbital (LUMO) and the highest occupied molecular orbital (HOMO) of the organic polymeric light emitting materials. This gives organic designers a lot of innovation space to tune the emitting light wavelength. Moreover, the emitting life time as well as the light emitting quantum efficiency and driving voltage of the electroluminescence (EL) performance are the key factors in evaluating the practical potential of the polymeric electroluminescence diode. In addition to aluminum (a popular metal in microelectronics), many other metals cathodes of low work function, such as Mg, Ca, Li or their alloys, have been widely used to enhance electron injection into the light emitting layer [5-7]. They can significantly improve the electroluminescence efficiency over several orders of magnitude and reduce the driving voltage. The light emitting quantum efficiency of PLEDs may also be promoted with many different methods. Primarily, they include inserting the electron (or hole) transport material between the light emitting layer and the metal cathode (or the indium tin oxide (ITO) anode), applying a tunnel layer in

*To whom all correspondence should be addressed.
Tel: 886-3-5731873; Fax: 886-3-5724727
E-mail: wtwhang@cc.nctu.edu.tw

J. Polym. Res. is covered in ISI (CD, D, MS, Q, RC, S), CA, EI, and Polymer Contents.

between, forming a heterojunction [8], blending the light emitting polymer with other polymers (the electron transport polymers or electronic inert polymers), and synthesizing new emitting materials with high electron affinity.

In addition, the processability of the electroluminescence polymer is also a factor of concern in PLEDs. Poly[2-methoxy-5-(2-ethylhexyloxy)-1,4-phenylene vinylene] (MEH-PPV), being an organic solvent soluble, has becomes a popular light emitting polymer. However, an amazing results have been reported in multilayer MEH-PPV LED [9,10]; although PMMA is an insulator, coating a thin PMMA layer (< 60 Å) on MEH-PPV with an aluminum cathode can improve the EL quantum efficiency without increasing the threshold voltage. The PMMA layer showed the tunnel effect but no explanation was put forth in this case. The electroluminescence quantum efficiency of MEH-PPV can also be improved by blending with other polymers. The improvement may be due to the electron affinity effect, the electron transport effect, or the dilute effect [11-17]. In polymer blends, the compatibility of different polymers affects the formation of domains and, in turn, affects the electroluminescence behavior. The morphology of the polymer blend is of critical importance to EL performance, yet the morphology of few MEH-PPV blends has been described.

Therefore, in this paper, we report on our attempts to blend PMMA into MEH-PPV in the light emitting layer to simplify the process and to improve the EL performance. A near-field scanning absorption microscope, a near-field scanning photoluminescence microscope, and an atomic force microscope were used to study the morphology and the surface distribution of the blend component and to link them with the EL performance. The electrical properties of thin PMMA films between Ca and ITO glass were also studied to more fully understand the mechanism of the so-called tunnel effect in PMMA thin film.

Experimental Section

1. Preparation of materials, polymer films, and light emitting diodes

PMMA (M_w = 130,000; M_w/M_n = 4.3) from Aldrich Inc. was used without further purification. MEH-PPV was synthesized by the method Hwang used [18,19] and it had a number-average molecular weight of 182,000 measured by GPC. The MEH-PPV and PMMA were dissolved together in toluene with various ratios. The polymer blend solution was spun on ITO glass at 1,000 rpm to give a film thickness of 800 Å and at 2,000 rpm to give a thickness of 400 Å. The polymer thin film was then vacuum dried in a high vacuum tube of 10^{-6} torr. The PMMA films for surface micrographs or X-ray diffraction measurement or I-V (current-voltage) curves were prepared by spin coating on glass plates at different speeds to give different film thicknesses and then vacuum dried at room temperature in a high vacuum tube of 10^{-6} torr. For studying the electrical properties of PMMA films, the PMMA solution in toluene was spin-coated on ITO glass plates. The films were also dried under a vacuum of 10^{-6} torr. For the orientation relaxation study, the vacuum dried PMMA films were aged at 120 °C for 12 hrs; calcium metal was then thermally coated on the polymer blend films or pure PMMA films to form Ca/blend/ITO LEDs or Ca/PMMA/ITO glass devices. The devices were protected by coating with a silver layer on the Ca surface.

2. Characterization

The I-V (current-voltage) curves of Ca/polymer blend/ITO LEDs and Ca/PMMA/ITO glass devices were measured with a Keithley 2400 instrument. Surface micrographs of PMMA films and the polymer blend films were recorded using a Burleigh ARIS-3300 atomic force microscope (AFM) with a standard Burleigh AFM probe. The scanning was performed at a constant force, typically 8.4 nN and the cantilever with a silicon pyramidal tip having a spring constant of ~0.05 N/m. The near-field scanning optical microscopy (NSOM) experiments were performed under ambient conditions using a near field scanning optical microscope with an optical fiber tip. To obtain a maximum optical contrast of the absorption micrographs, the NSOM was operated at the wavelength 590 nm, which was near the UV-Vis absorption peak of MEH-PPV, while the PMMA had a negligible absorption at this wavelength. For fluorescence micrographs, the NSOM was operated at a wavelength which was 320 nm of the UV light. X-ray diffraction spectra of spin-coated PMMA films were measured by a Mac Science M18 X-ray diffractometer (50 KV, 250 mA) with a copper target and Ni filter at a scanning rate of 4°/min.

Results and Discussion

The dependence of electroluminescence performance of current versus voltage (I-V) on the composition of MEH-PPV/PMMA blends in Ca/polymer/ITO LEDs is shown in Figure 1. The threshold voltages (V_{th}) of the LEDs are 5.5, 3.9, and 2.9 Volts, the light emitting layer being MEH-PPV, MEH-PPV/

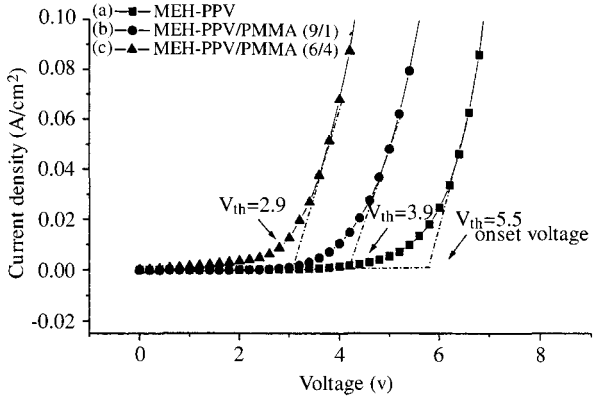

Figure 1. Current density dependence on voltages in LEDs of (a) Pristine MEH-PPV (■), (b) MEH-PPV/PMMA (9/1) (●), and (c) MEH- PPV/PMMA (6/4) (▲).

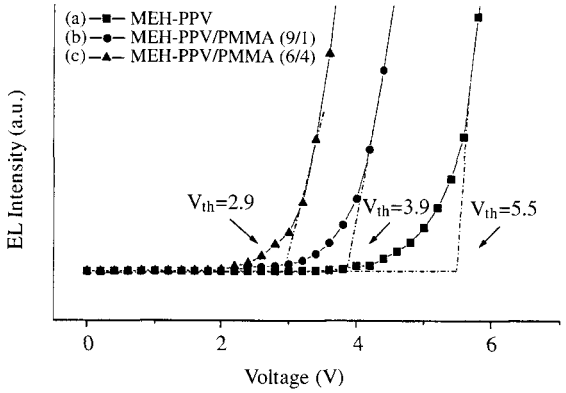

Figure 2. Electroluminescence intensity dependence on voltages in LEDs of (a) pristine MEH-PPV (■), (b) MEH-PPV/PMMA (9/1) (●), and (c) MEH- PPV/PMMA (6/4) (▲).

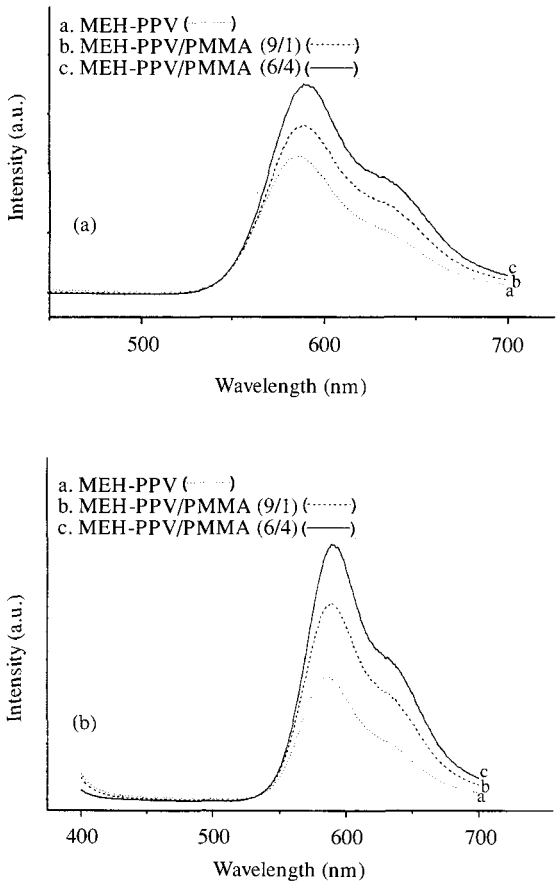

Figure 3. (a) PL spectra and (b) EL spectra of pristine MEH-PPV (....) and MEH-PPV/PMMA blends (9/1, ...) and (6/4, —).

PMMA (9/1), and MEH-PPV/PMMA (6/4) respectively. The V_{th}, significantly decreases with the addition of PMMA content in the light emitting layer, although the PMMA is non-conjugated and insulated. The forward current also increases with the increase in PMMA content. The dependence of electroluminescence intensity on the drive voltage in Figure 2 exhibits the same V_{th} value as in Figure 1. At the same drive voltage, the MEH-PPV/PMMA blend LEDs have much higher brightness than the pristine MEH-PPV LED, and the EL brightness of MEH-PPV/PMMA (6/4) LED is much higher than that of MEH-PPV/PMMA (9/1) under the same conditions. The EL brightness strongly depends on the ratio of the two components. The higher the PMMA content in the light emitting layer, the greater the EL brightness of the blend LED.

Figure 3 shows the photoluminescence and electroluminescence spectra of MEH-PPV and MEH-PPV/PMMA blends. The emission peak of the pristine MEH-PPV EL spectrum occurs at around 590 nm with a shoulder at 615 nm. The EL spectra of the polymer blends MEH-PPV/PMMA (9/1) and (6/4) do not change with the blend ratio. The EL spectra are similar to their PL spectra, meaning that blending PMMA into MEH-PPV does not alter the energy gap of MEH-PPV. Therefore, no complex or exciplex formation occurs in these two blends.

A near-field scanning optical microscope (NSOM) was used to examine the domain distribution on the polymer surface. Each NSOM experiment was accompanied by an atomic force microscope (AFM) experiment under the same ambient conditions, as shown in Figures 4 and 5. Figures 4(b), 4(d), 5(b), and 5(d) are the atomic force micrographs of the blends MEH-PPV/PMMA (9/1) and (6/4). The corresponding near-field scanning absorption micrographs and photoluminescence micrographs are shown in Figures 4(a), 4(c), 5(a), and 5(c), respectively. To maximize the optical contrast of the absorption micrographs, the near-field scanning was performed with an optical beam of wavelength 590 nm, which is near the absorption peak of

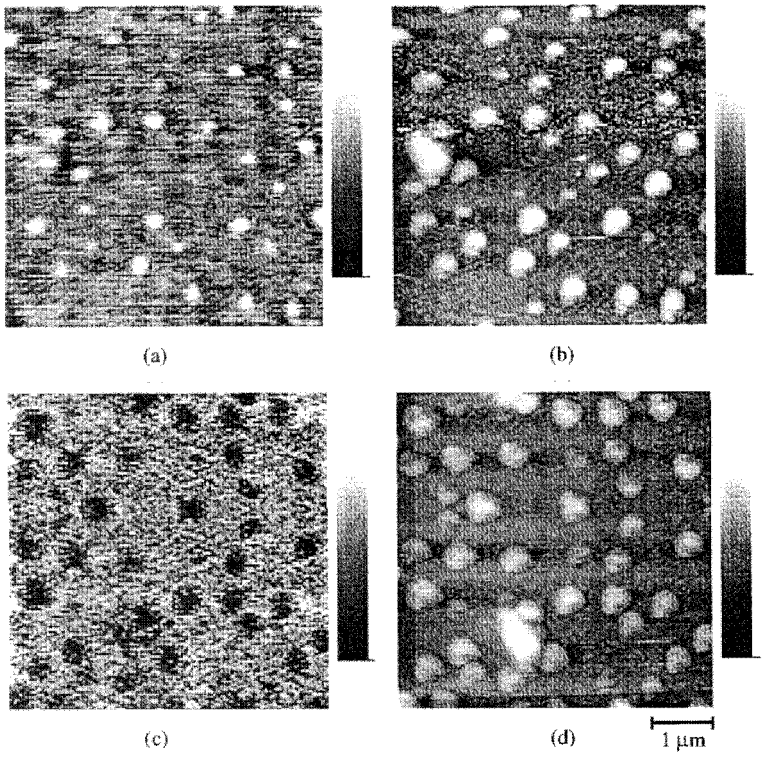

Figure 4. Surface domain micrographs of MEH-PPV/PMMA (9/1): (a) near field scanning absorption micrograph, (b) corresponding atomic force micrograph, (c) near field scanning photoluminescence micrograph, and (d) corresponding atomic force micrograph.

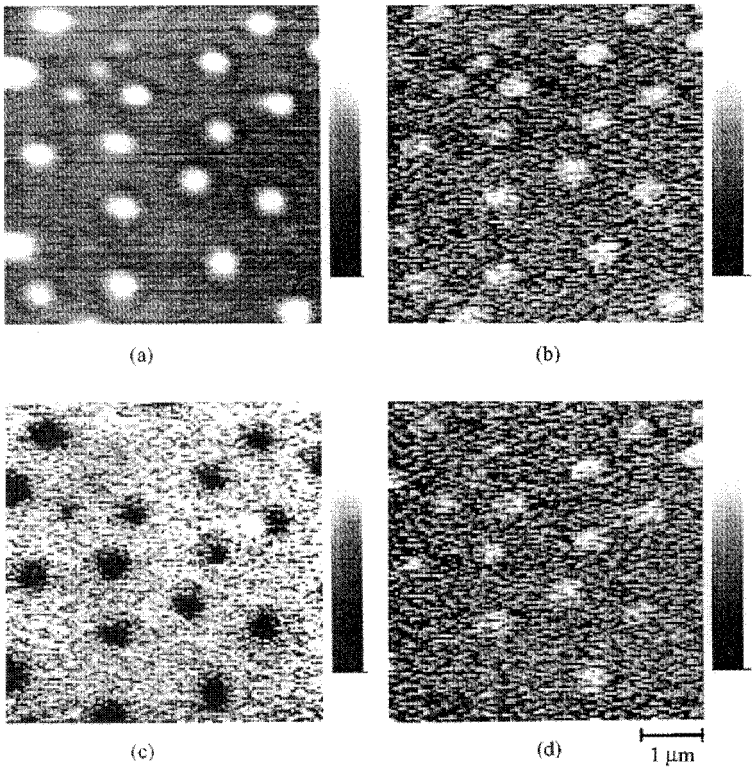

Figure 5. Surface domain micrographs of MEH-PPV/PMMA (6/4): (a) near field scanning absorption micrograph, (b) corresponding atomic force micrograph, (c) near field scanning photoluminescence micrograph, and (d) corresponding atomic force micrograph.

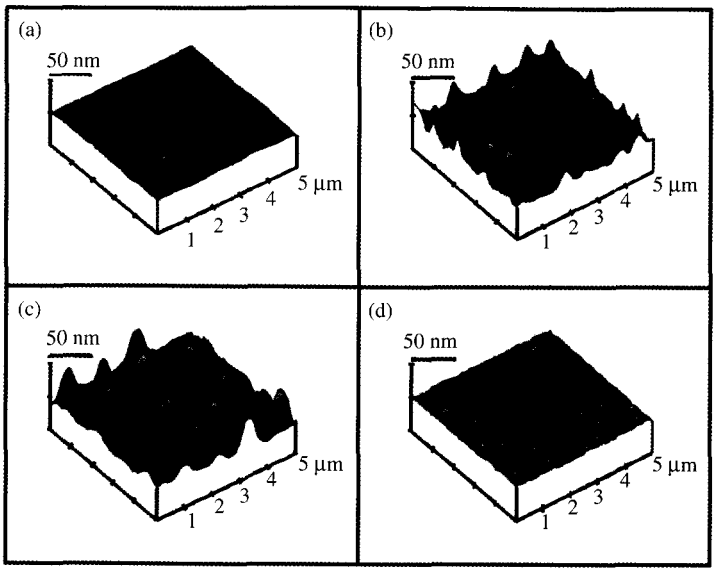

Figure 6. Surface topography of polymer films: (a) MEH-PPV, (b) MEH-PPV/PMMA (9/1), (c) MEH-PPV/PMMA (6/4), and (d) PMMA by atomic force microscope (X axis: 1.0 μm/div; Z axis: 50 nm/div).

MEH-PPV, since PMMA has negligible absorption at this wavelength. Figures 4(a) and 5(a) show the topographic absorption images of the thin film (800A in thickness) of these two blends. The bright areas are the PMMA domains. Both figures exhibit the PMMA domains dispersed in the MEH-PPV continuous phase. The PMMA domain size increases with the PMMA content in the blend. In order to confirm the result, we performed near-field scanning photoluminescence experiments. The photoluminescence micrographs are shown in Figures 4(c) and 5(c). The bright areas of the photoluminescence micrographs are of the MEH-PPV domains, while the dark areas (no photoluminescence) correspond to the PMMA phase. They also show the PMMA domain size increasing with the PMMA content.

To obtain the three dimensional topographies of the polymer thin films, a high efficiency AFM was performed in the surface scanning experiment. The AFM surface micrographs are shown in Figures 6(a)-6(d) for the films of MEH-PPV, MEH-PPV/PMMA (9/1), MEH-PPV/PMMA (6/4), and PMMA, respectively. The film surfaces of the pristine MEH-PPV and pristine PMMA are fairly smooth as shown in Figures 6(a) and 6(d). Figures 6(b) and 6(c) show a rough surface and the surface roughness increases with the PMMA content. It seems that blending PMMA into MEH-PPV causes an increase in the film roughness. In Figures 6(b) and 6(c), the PMMA domains, growing out of the blend film surface, appear to like bamboo shoots on the topography. In MEH-PPV/PMMA (9/1), the average PMMA shoot height is about 100 Å and the average domain ground surface diameter about 0.4 μm. In MEH-PPV/PMMA (6/4), the average PMMA shoot height is about 200 Å and the average domain ground surface diameter about 0.8 μm.

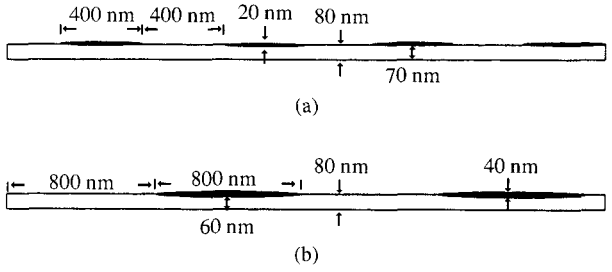

Figure 7. Surface topography of equal scale ratio on X- and Z-axes for MEH-PPV/PMMA films (a) (9/1) and (b) (6/4).

In the two dimensional image of the two blends at the same ratio of real scale to represent the image, the PMMA domains in the blend may appear rather like "sesame seeds embedded on the surface of a pancake" as shown in Figure 7. If the PMMA domains are symmetrically embedded on the surface of the blend thin film, this means that the other equal half of each PMMA domain is embedded under the surface. Because MEH-PPV is a continuous phase and PMMA a dispersed phase, the PMMA domains may cover about one quarter of the ground surface area of the blend thin film if each MEH-PPV and PMMA section occupies equal length in one dimensional cross section. The MEH-PPV flat surface area may cover three quarters of the ground surface area of the blend thin film, so it is reasonable to suppose that the film thickness is measured from

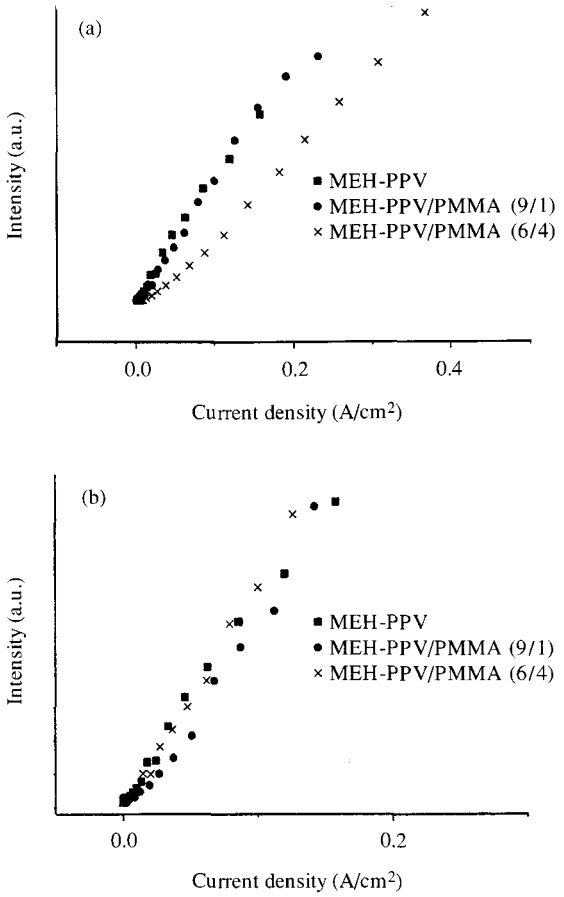

Figure 8. Relative EL intensity normalized with MEH-PPV ratios for (a) MEH-PPV and (b) MEH-PPV/PMMA blend LEDs.

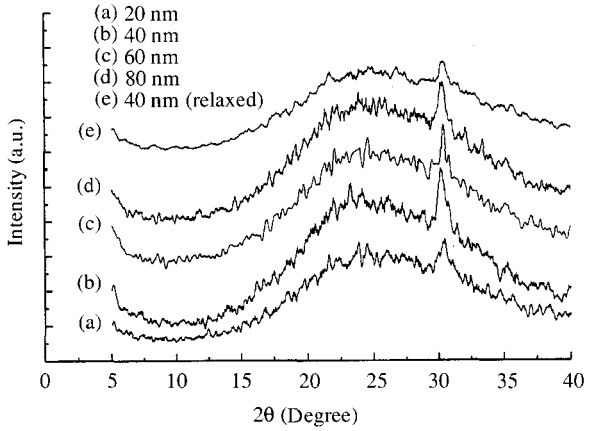

Figure 9. Dependence of XRD spectra on film thickness for spin-cast and relaxed PMMA films.

the ground surface to the ITO surface. How does the morphology of the blend film affect its electroluminescence characteristics? In many cases, inert polymers blending with a light emitting polymer can improve the electroluminescence efficiency with or without increasing the threshold voltage. Many cases are due to the so-called "dilute effect", which is attributed to enlarging the separation of the light emitting molecular chain and reducing the non-radiative interaction of excitons. Therefore, the radiative relaxation of excitons increases and the EL quantum efficiency is promoted. Usually, the dilute effect does not cause a reduction in the threshold voltage. In this paper, the threshold voltage of Ca/blend/ITO LEDs decreases with the PMMA content, a result quite different from that reported in the literature. Therefore, we have examined carefully the effect of the PMMA content on the electroluminescence efficiency. In Figure 8 the slope of each curve relates to the EL efficiency and the EL light intensity per unit current. In Figure 8(a) the apparent EL efficiency decreases with the PMMA content, meaning that the higher the PMMA content, the lower the apparent EL light intensity per unit current. Because PMMA is not a light emitting material, the apparent EL intensity should be normalized with the MEH-PPV ratio in the emitting layer to obtain the real EL efficiency per unit MEH-PPV chromophore in the blends. As shown in Figure 8(b), the MEH-PPV chromophores in the pristine MEH-PPV, or MEH-PPV/PMMA (9/1)), or MEH-PPV/PMMA (6/4) have almost equal EL efficiencies. No dilute effect was found in these two blends. However how can we then explain that the threshold voltages decrease when the PMMA content in the blends increases ?

PMMA is an amorphous polymer. Usually, no X-ray peak, only a broad curve is found in bulk PMMA. However, in Figure 9, there is a peak at $2\theta = 30.3°$ in each X-ray spectrum for spin casting PMMA film of 200, 400, 600 and 800 Å thicknesses after vacuum drying. If the film is relaxed for 6 hrs after spin casting, the X-ray peak decreases dramatically. Apparently the X-ray peak at $2\theta = 30.3°$ results from the molecular chain orientation. The peak height, which depends on the film thickness increases from the 200 Å to the 400 Å films and the decreases from the 400 Å to the 800 Å films. The X-ray peak at $2\theta = 30.3°$ corresponds to a repeat distance of 2.946 Å. In Jou's paper [20], polyimide films showed a dependence of orientation and ordering on the film thickness. In our study, the thinner film had a better film orientation for the spin casting polyimide film of thickness 2.2 to 11.3 μm. The lower X-ray intensity of 200 Å PMMA film in Figure 9 may be due to the thinner film causing less effective diffraction, not due to a poorer orientation. It is also true that the thinner film had better orientation and ordering in these PMMA films. Figure 10 shows the dependence of the I-V curves on the PMMA and MEH-PPV film thickness. The

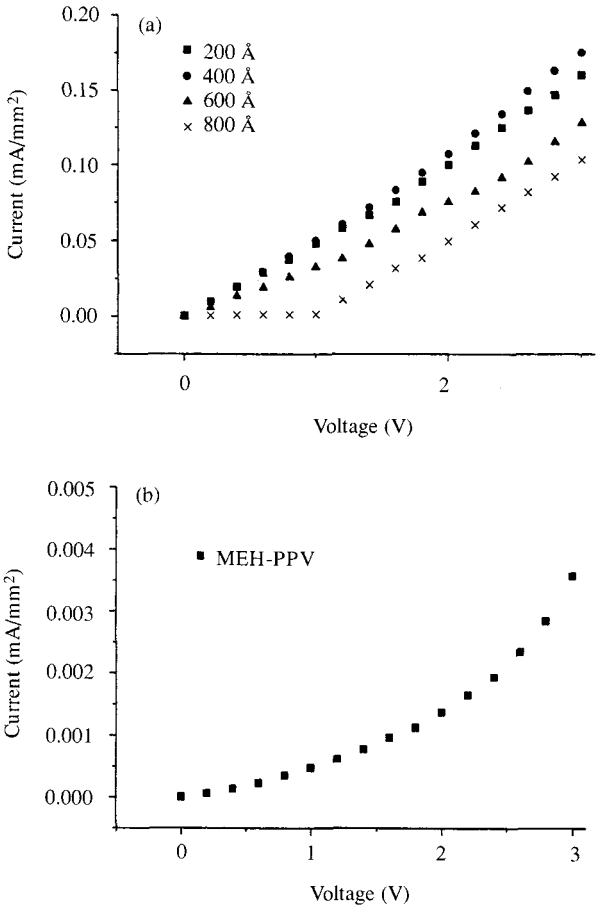

Figure 10. (a) Dependence of I-V curves on PMMA thickness in Ca/PMMA/ITO glass devices for the vacuum dried PMMA and (b) the I-V curve of Ca/MEH-PPV/ITO glass devices for the vacuum dried MEH-PPV.

Table I. The resistance R and resistivity ρ of thin PMMA and MEH-PPV films in Ca/PMMA or MEH-PPV/ITO glass devices for the vacuum dried PMMA and MEH-PPV.

Thickness (Å) \ Properties		Resistance (R, Ω·m²)	Resistivity (ρ, Ω·m)
PMMA	200	1.7×10^{-2}	8.6×10^{5}
	400	1.9×10^{-2}	4.7×10^{5}
	600	2.4×10^{-2}	3.8×10^{5}
	800	2.6×10^{-2}	3.3×10^{5}
MEH-PPV	800	1.5	1.8×10^{7}

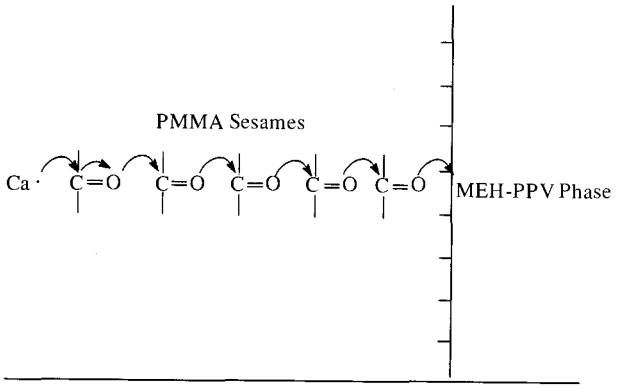

Figure 11. Proposed electron hopping mechanism in PMMA.

resistance and resistivity of the films are shown in Table I. The data indicate that thin PMMA films have much lower resistivity than the MEH-PPV. The former even shows two orders of resistivity lower than the latter. Moreover, the PMMA films have a linear I-V relationship and an ohmic-contact behavior, but the MEH-PPV has neither. Apparently, thin PMMA films and MEH-PPV film have different electrical characteristics. It is well known that the hole mobility in the conjugated polymer is usually faster than the electron mobility, except that the introduction of electron transport units easily causes an imbalance between the holes and the electrons in the light emitting polymer. Therefore, balancing the holes and electrons in the light emitting polymer can significantly improve the electroluminescence efficiency and threshold voltage by adjusting the interface barrier for the both holes and the electrons, as Parker claims [7]. The reduction of the V_{th} in the LED of the MEH-PPV/PMMA blend is related to the much lower resistivity of PMMA.

In PMMA, we believe the conduction is mainly due to electron transport, not hole transport because aldehyde-containing monomers can be polymerized to form polyether through anion polymerization in the presence of a strong base, but not through cationic polymerization.

The resistance of the PMMA films increases with the film thickness, but the resistivity decreases with the film thickness. For a thin film, the pin-hole defect density increase with decreasing film thickness [21]. The pin-hole defects may cause the deposition of Ca and promote the conductivity. Therefore, if the thin PMMA conductivity is due to the pin-hole mechanism, the resistivity of the film should increase with the film thickness. But the situation is actually reversed. Therefore, the thin PMMA conductivity may go through other mechanism. We propose that the conduction starts from the low work function metal calcium atom releasing $\overset{\curvearrowright}{Ca\cdot}\overset{\curvearrowright}{C=O}$ electron to the carbon atom and through oxygen atom of the carbonyl group under an electrical field, and the electron hopping from one carbonyl group to other carbonyl groups, as shown in Figure 11. The electron hopping through carbonyl groups does not cause polymerization because of the two bulky groups on the carbon atom.

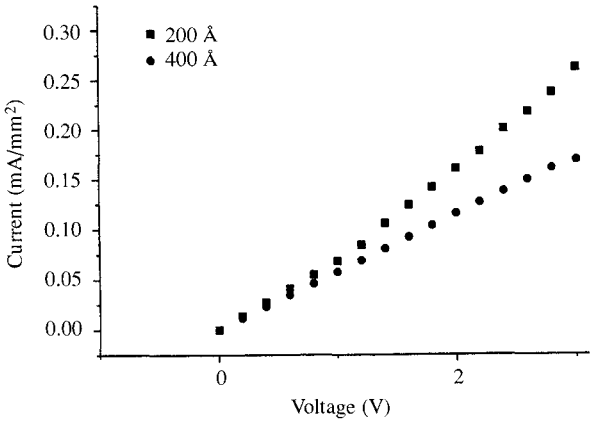

Figure 12. Dependence of I-V curves on PMMA thickness in Ca/PMMA/ITO glass devices for the PMMA film baked at 120 °C for 12 hrs.

If one or the bulky groups is replaced with a hydrogen atom, then reaction (or polymerization) may occur. This really does occur in aldehyde compounds as anionic polymerization in the presence of strong bases, but not for ketones [22]. Here, the carbonyl groups may cause electron transport but not reaction because of the two bulky groups on both sides of the carbon atom. The orientation of the PMMA film puts the carbonyl groups in order and keeps them far away from each other. But the disoriented carbonyl groups, intermolecular or intramolecular, are free to more closer to each other due to the dipole-dipole interaction. Hence the resistivity decreases with increasing the film thickness. The disorientation favoring the electron hopping is also shown in Figure 12 and Table II. When PMMA film is baked at 120 °C for 12 hrs to relax the molecular chain orientation after vacuum drying, the resistivity of PMMA decreases as shown in Figure 12 and Table II. The disorientation favors electron hopping. Therefore, the decrease in the V_{th} of the MEH-PPV/PMMA blend LED with the PMMA content can be assumed to be due to the electron hopping through the thin PMMA "sesame seeds" in the electrical field and also due to the less effective MEH-PPV thickness. The higher the PMMA content, the thinner the effective MEH-PPV layer in the blend and the lower the electrical field needed to trigger electroluminescence.

Conclusion

A novel method for improving the driving voltage of MEH-PPV is presented by blending with PMMA. The V_{th} decreases with the PMMA content. With the MEH-PPV/PMMA blend, the V_{th} of the polymer LED is only 2.9 volts, reduced from the 5.4 volts of the pristine MEH-PPV LED. The near-field scanning absorption and photoluminescence micrographs show the PMMA domains dispersed in the continuous MEH-PPV phase like sesame seeds embedded in a pancake. No dilute effect was found in the electroluminescence performance. Blending does not change the EL efficiency of MEH-PPV. The resistivity of the PMMA films is much lower than that of the MEH-PPV film in the ITO/polymer/Ca devices. The resistance of thin PMMA film in Ca/PMMA/ITO glass devices increases with the film thickness, but the resistivity decreases with increasing the film thickness. Therefore, the excellent conduction of PMMA is not due to the pinhole defect mechanism but results from the electron hopping from Ca to the carbon atom and through the oxygen atom of the first carbonyl group and then hopping to the neighboring carbonyl groups. The electron hopping can be both intramolecular and intermolecular. Therefore, the decrease in the driving voltage of the Ca/polymer/ITO LEDs may be due to the electron hopping through the carbonyl groups of the PMMA sesame seeds in the MEH-PPV/PMMA light emitting layer as well as the thinner effective MEH-PPV thickness.

Table II. Resistance R and resistivity ρ of thin PMMA film in Ca/PMMA/ITO glass devices for the PMMA film baked at 120 °C for 12 hrs.

Thickness (Å) \ Properties	Resistance (R, Ω·m²)	Resistivity (ρ, Ω·m)
200	1.2×10^{-2}	5.7×10^{5}
400	1.7×10^{-2}	4.3×10^{5}

Acknowledgement

The authors gratefully acknowledge the financial support of the National Science Council of the Republic of China and the Lee and MTI Center for Networking Research for work under Grant NSC. 88-2216-E-009-058 and the Photonic Devices and Mualules Project respectively. The authors also appreciate the kind assistance of Pei-Kuen Wei for his near-field scanning optical microscope measurements.

References

1. J. H. Burroughes, D. D. C. Bradley, A. R. Brown, R. N. Marks, K. Mackay, R. H. Friend, P. L. Burns and A. B. Holmer, *Nature*, **347**, 539 (1990).

2. A. Kraft, A. C. Grimsdale and A. B. Holmes, *Angew. Chem., Int. Ed. Engl.*, **37**, 402 (1998).
3. N. C. Greenham, S. C. Moratti, D. D. C. Bradley, R. H. Friend and A. B. Holmes, *Nature*, **365**, 628 (1993).
4. I. Sokolik, Z. Yang, F. E. Karasz and D. C. Morton, *J. Appl. Phys. Commun.*, **75**, 35842 (1993).
5. D. Braun and A. J. Heeger, *Appl. Phys. Lett.*, **58**, 1982 (1991).
6. S. Aratani, C. Zhang, K. Pakbaz, S. Hoger, F. Wedle and A. J. Heeger, *J. Electron. Mater.*, **22**, 745 (1994).
7. I. D. Parker, *J. Appl. Phys.*, **75**, 1656 (1994).
8. G. E. Jabbour, B. Kippelen, N. R. Armstrong and N. Peyghambarian, *Appl. Phys. Lett.*, **73**, 1185 (1998).
9. Y. E. Kim, H. Park and J. J. Kim, *Appl. Phys. Lett.*, **69**, 599 (1996).
10. Y. E. Kim, H. Park and J. J. Kim, *Synth. Met.*, **85**, 119 (1997).
11. J. I. Lee, I. N. Kang, D. H. Hwang and H. K. Shim, *Chem. Mater.*, **8**, 1925 (1996).
12. H. K. Shim, H. J. Kim, T. Ahn, I. N. Kang and T. Zyung, *Synth. Met.*, **91**, 289 (1997).
13. I. N. Kang, D. H. Hwang, H. K. Shim and T. Zyung, *J. Kim, Macromolecules*, **29**, 165 (1996).
14. H. K. Shim, I. N. Kang, M. S. Jang, T. Zyung and S. D. Jung, *Macromolecules*, **30**, 7749 (1997).
15. J. Y. Park, H. M. Lee, G. T. Kim, H. Park, Y. W. Park, I. N. Kang, D. H. Hwang and H. K. Shim, *Synth. Met.*, **79**, 177 (1996).
16. S. Aratani, C. Zhang, K. Pakbaz, S. Hoger and F. Wudl, A. J. Heeger, *Appl. Phys. Lett.*, **61**, 2793 (1993).
17. C. Zhang, S. Hoger, K. Pakbaz, F. and A. J. Heeger, *J. Electron. Mater.*, **23**, 453 (1993).
18. G. Krausch, C. A. Dai, E. J. Kramer, J. F. Marko and F. S. Bates, *Macromolecules*, **26**, 5566 (1993).
19. D. H. Hwang, S. T. Kim, H. K. Shim, A. B. Holmes, S. C. Moratti, AND R. H. Friend, *J. Chem. Soc. Chem. Commun.*, **19**, 2241 (1996).
20. J. H. Jou and P. T. Hwang, *Macromolecules*, **24**, 3796 (1991).
21. A. M. Wilson, D. Larks and S. M. Daris, ACS symposium series 184, chap. 11, p. 143, American Chemical Society, Washington D.C., 1982.
22. G. Odian, *Principles of polymerization*, 3rd. John Wieley & Sons. New York, 1981.